

PACS numbers: 87.15.Vv; 87.64.Cc
DOI: 10.1070/QE2014v044n07ABEH015544

Study of diffusion of indocyanine green as a photodynamic dye into skin using backscattering spectroscopy

E.A. Genina, A.N. Bashkatov, V.V. Tuchin

Abstract. **One of the lines of development of modern medicine is theranostics consisting in simultaneous diagnosis and laser treatment with the use of multifunctional agents such as fluorescent indocyanine green that has photodynamic and photothermal properties. Diffusion of indocyanine green dissolved in water and aqueous solutions of alcohols (glycerol, propylene glycol and ethanol) into the dermis is studied by using backscattering spectroscopy. The coefficients of the dye diffusion into the dermis are obtained for the first time by using these solvents.**

Keywords: *indocyanine green, dermis, backscattering spectroscopy, diffusion coefficient.*

1. Introduction

One of the new trends in modern medicine is the development of theranostic methods for simultaneous imaging of the object and its photodynamic and/or photothermal therapy using multifunctional agents [1,2]. For precise localisation of tumours hidden deep in biological tissue, use is made either of inhomogeneity contrast enhancement (which is achieved by the introduction of exogenous dyes or nanocomposites with a fairly narrow absorption band in the visible or near-IR spectral range [3–5]) or fluorescence [3,6]. For selective removal of tumours, these agents must simultaneously possess photodynamic and/or photothermal properties [5,7,8].

In this regard, one of the most promising dyes for use in theranostics is indocyanine green (ICG). The literature contains reports of the use of this fluorescent dye for diagnostic purposes in studies of the functions of heart and liver [9], in retinal and choroidal angiography [10,11], in tumour imaging [3] and for estimating the depth of thermal lesions [12], as well as in many other applications. Indocyanine green, administered intravenously, is bonded with plasma proteins and circulates through the vascular system. Binding and spectral properties of ICG make it possible to develop new imaging system for surgery, particularly for plastic and reconstructive surgery, neurosurgery, oncology, and many other applications [13–15]. Besides, ICG has well-pronounced photodynamic [16,17], phototoxic [18] and photothermal properties [19,20], allowing its effective use in laser therapy and surgery.

Indocyanine green (4,5-benzoindotricarbocyanine) is a nontoxic tricarbocyanine dye. The chemical formula of ICG is $[C_{43}H_{47}N_2O_6S_2]^{2-}\cdot 2Na^+$, and the molecular weight is 775. The dye is a water-soluble anionic photosensitizer [16]. According to the literature, ICG solubility in distilled water is no more than 5 mg mL^{-1} [21]. Solubility of ICG in physiological saline is much lower than that in water, causing aggregation and sedimentation of the dye at a concentration from 0.01 to 1 mg mL^{-1} [22]. Alcohols, on the contrary, significantly increase ICG solubility. As shown in [22], if the ratio of water and alcohols is no less than 1:1, alcohols start playing the key role. An increase in the concentration of water in the mixture leads to a sharp increase in the degree of aggregation of dye molecules [23]. ICG has affinity to blood proteins (primarily to albumin [13]) and biological tissues [23,24].

ICG has a strong absorption band in the red and near-IR regions of the spectrum (700–800 nm). In this range there are two absorption bands: the short-wavelength band is located in the red or near-IR region of the spectrum (690–730 nm), whereas the long-wavelength band (770–790 nm) lies in the near-IR region. To this end, the long- and short-wavelength bands correspond to the absorption of the dye monomer and dimer, respectively. In aqueous solutions of the dye, dimerisation has been observed at concentrations of 10^{-7} mol cm^{-3} [14].

When interacting with a biological tissue the absorption band maxima of ICG monomers shift to longer wavelengths [11,23,24].

At high concentrations, the dependence of the efficiency of light absorption by the dye on its concentration is nonlinear, because in this case, the dye has a tendency to aggregate in larger particles in water and aqueous salt solutions of NaCl. So-called J-aggregates are threadlike compounds of monomer molecules. The absorption band of ICG J-aggregates lies in the region of 890 nm [25, 26]. The intensity and position of the absorption bands and their mutual ratio depend on the solvents used [27].

From the viewpoint of improving the interaction between optical radiation and the dye sensitizing a biological tissue, quite promising may be a simultaneously staining of the biological tissue in question and reduction of its light scattering (as it will provide a greater depth of radiation penetration), which can be achieved by using dye solutions in immersion agents.

E.A. Genina, A.N. Bashkatov Research and Educational Institute of Optics and Biophotonics, N.G. Chernyshevsky Saratov State University, ul. Astrakhanskaya 83, 410012 Saratov, Russia; e-mail: eagenina@yandex.ru, a.n.bashkatov@mail.ru;
V.V. Tuchin Research and Educational Institute of Optics and Biophotonics, N.G. Chernyshevsky Saratov State University, ul. Astrakhanskaya 83, 410012 Saratov, Russia; Institute of Problems of Precision Mechanics and Control, Russian Academy of Sciences, ul. Rabochaya 24, 410028 Saratov, Russia; University of Oulu, P.O. Box 4500, Oulu FIN-90014, Finland; e-mail: tuchinvv@mail.ru

Received 10 April 2014; revision received 17 May 2014
Kvantovaya Elektronika **44** (7) 689–695 (2014)
Translated by I.A. Ulitkin

However, despite a large number of publications on the use of ICG, studies of the diffusion rate of this dye in biological tissues are scarce and peculiarities of its interaction with biological tissues remain poorly understood, mainly when hyperosmotic immersion liquids are used as solvents. Employment of alcoholic solutions as ICG diffusion amplifiers requires a more detailed investigation.

The aim of this paper is to study the interaction of ICG with the dermis during its diffusion by using aqueous solutions of the dye and ICG solutions in ethanol, propylene glycol and glycerol, and to determine the coefficient of ICG diffusion into the dermis.

2. Materials and Methods

In the experiments we used ICG (Aldrich Chemical Co., USA) in the following solvents: distilled water, 50% aqueous solution of ethanol, 50% aqueous solution of glycerol (CJSC 'Baza No. 1 Khimreaktivov', Russia), 50% aqueous solution of propylene glycol (JSC 'Reaktiv', Russia). The ICG concentration in all the solutions was 1 mg mL^{-1}, which corresponds to the dye concentration often used for both diagnostic [28] and therapeutic purposes [29, 30].

To measure the absorption coefficients of the solutions in question, we used a double-beam CARY-2415 spectrophotometer (Varian, Australia) with an integrating sphere in the regime of total transmittance in the 400–1000 nm spectral range. The inner diameter of the sphere was 100 mm, the size of the entrance opening was 20×20 mm, and the diameter of the exit opening was 16 mm. As a light source we used a halogen lamp filtering radiation in the spectral range under study. The diameter of the light beam incident on the cuvette with the solution was 3 mm and the thickness of the cuvette was 30 μm. Measurements were carried out with the corresponding solvents, the cuvette with which was placed in a comparison channel. All experiments were performed at room temperature (~20 °C).

The samples for the study of diffusion of ICG solutions into biological tissue were extracted by autopsy from the skin of outbred white laboratory rats. Before the experiment the subcutaneous fat layer and hair were thoroughly removed. The thickness of the samples ranged from 0.6 to 1 mm.

The reflectance was measured with an optical multichannel LESA-5 analyser (Biospec, Russia). A sample of skin with the epidermis on the outside was attached to the opening of the cylindrical cuvette pre-filled with a test solution. The cuvette was secured horizontally in a rack, so that the solution comes into contact with the sample surface. A fibre-optic probe of the device was mounted on the opposite surface of the sample (see Fig. 1). The fibre-optic probe consisted of seven fibres with the central fibre delivering incident light into biological tissue; other six fibres – symmetrically arranged around the central fibre – collected the light scattered by the sample of biological tissue in the opposite direction. The diameter of each fibre was 200 μm, and the distance between the centres of the delivering and receiving fibres was 280 μm. The source of radiation in the spectral range from 450 to 1000 nm was a halogen lamp. The signal acquisition time was 100 ms.

The sample was secured so that the dye penetrated into the tissue from the dermis, and spectra of backscattered signals were measured from the side of the epidermis. To prevent dehydration of the skin sample in the experiment, it was

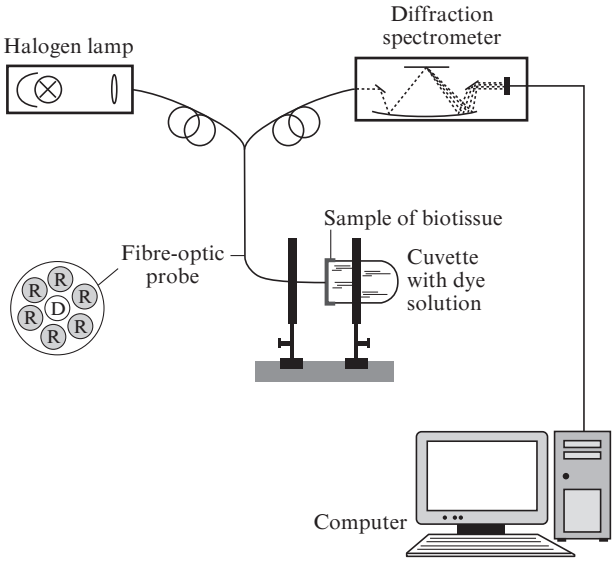

Figure 1. Scheme of the experimental setup (R – receiving fibre, D – delivering fibre).

covered with Parafilm M (American National Con., USA) on the outside, excluding the area in contact with the fibre-optic probe.

The backscattering coefficient (reflectance) of skin was measured for 2 to 8 hours before the termination of the changes in the reflectance spectra. The measured reflectance spectra were used to calculate the spectra of the effective optical density (EOD) $A(\lambda)$ with the help of the relation [31]

$$A(\lambda) = -\ln[R(\lambda)], \tag{1}$$

where $R(\lambda)$ is the time-dependent reflectance measured experimentally and λ is the wavelength (in nm). The $A(\lambda)$ parameter is widely used in biological tissue optics to study diffuse reflectance of skin *in vivo* [31–35].

To quantify changes in the content of the dye in biological tissue and to determine the diffusion coefficient, the authors of [31, 36] applied a method based on the use of the modified Beer–Lambert–Bouguer law. According to this method, the EOD of a biological tissue is

$$A = \mu_a \sigma \rho + G, \tag{2}$$

where μ_a is the absorption coefficient (in cm^{-1}); ρ is the distance between the source and the detector of backscattered radiation (in cm); σ is differential photon path length factor, taking into account the extension of the trajectory of the detected photons due to multiple scattering; and G is a constant determined by the geometry of the medium and experiment.

Given equation (2), the EOD of the skin sample measured at different times during penetration of the dye into biological tissue was determined as follows [37, 38]:

$$A(t, \lambda) = A(t = 0, \lambda) + \Delta\mu_a(t, \lambda)\rho\sigma, \tag{3}$$

where t is the time (in s); $\Delta\mu_a(t,\lambda) = \alpha(\lambda)C(t)$ is the difference between the absorption coefficients of biological tissue at each instant of time and the initial instant of time, actually determining the absorption coefficient of the dye inside biological tissue (in cm^{-1}); $\alpha(\lambda)$ is the molar absorption coefficient of the dye ($cm^2\ mol^{-1}$); $C(t)$ is the molar concentration of the dye in biological tissue (mol cm^{-3}); and $A(t=0,\lambda)$ is the EOD of the sample, measured at the initial time before its staining.

The diffusion coefficient D was determined by minimising the objective functional:

$$f(D) = \sum_{i=1}^{N_t} [\Delta A(D,t_i) - \Delta A^*(t_i)]^2, \quad (4)$$

where N_t is the total number of experimental points obtained by recording the reflectance dynamics at a fixed wavelength; $\Delta A(D,t)$ is the EOD, calculated at a time t for a given value of D; and $\Delta A^*(t)$ is the experimentally measured value of the EOD at a time t. More details on this method are presented in [37, 38].

3. Results and discussion

Figure 2a shows the ICG absorption spectra measured in various solvents. The ICG solution in 50% propylene glycol has the highest absorption coefficient (1142 cm^{-1}) in the examined wavelength band. The lowest absorption coefficient (252 cm^{-1}) with the same dye concentration is observed in the aqueous solution of ICG. Figure 2b presents the ICG absorption spectra normalised to the maximum value of the ICG absorption coefficient in the solutions under study (μ_a^{norm}). It is clearly seen that at equal concentrations of ICG in all the solutions, dimers predominate in aqueous solvents, which is evidenced by an increase in μ_a^{norm} at a wavelength of 697 nm as compared with a wavelength of 769 nm. The absorption spectra of the alcohol solutions of ICG (glycerol, propylene glycol and ethanol) exhibited a growth of μ_a^{norm} around 788 nm and a decrease around 724 nm, indicating a predominance of monomers in the dye solution. Both absorption maxima are shifted to the IR region of the spectrum.

It is known that the position of the absorption bands and the ratio of their amplitudes determined by the presence of monomers and dimers in the dye solution depend on the nature of the solvent. Differences in the spectra characterise the efficiency of heterogeneous association of ICG molecules in different solvents. It follows from Fig. 2 that the efficiency is the highest in the case when the solvent is water, followed by glycerol, propylene glycol and ethanol in descending order.

The reasons for this effect are, first, the differences in the values of the dielectric constant ε for different solvents [39]. Typically, dye molecules in solutions exist in the form of charged ions, whereby the relative dielectric constant of the solvent exerts a great influence on the process of association. For the solvents in question at 20 °C, ε takes the following values: 80.4 (water) [40], 56.2 (glycerol) [40], 32 (propylene glycol) [41] and 27.8 (ethanol) [40]. With decreasing ε, the efficiency of heterogeneous association of the dyes is reduced. Moreover, molecules of various solvents are differently oriented around dye molecules, resulting in formation of different solvation shells, which affect both the absorption properties of the dye and the efficiency of its dimerisation. Finally, the spectral characteristics of the dye in different solvents may vary in the interaction of molecules; as a result, hydrogen bonds form between them [39].

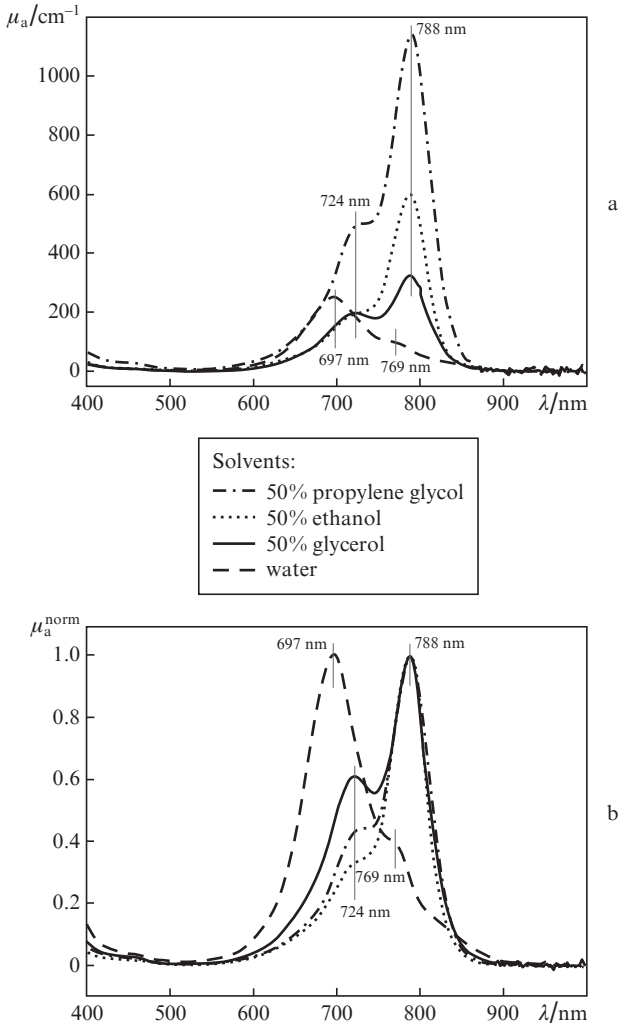

Figure 2. Spectra of (a) the absorption coefficient and (b) normalised absorption coefficient of ICG solutions in different solvents. The ICG concentration in all the solutions is 1 mg mL^{-1}.

An increase in the absorption coefficient in the short-wavelength region of the visible spectrum corresponds to the edge of a low peak near 400 nm, as observed in the spectra of monomeric and dimeric forms of ICG. The solutions of dye monomers have a higher peak near 200 nm, whereas for dimers such a peak is absent [42]. In the wavelength range above 890 nm, the absorption coefficient of solutions is close to zero, indicating the absence of aggregation of ICG molecules in all the solutions under study.

Figure 3 shows a sample sequence of EOD spectra of skin during its interaction with the ICG solutions in question. The time of the study was determined by the termination of the changes in the shape of the spectrum and signal level.

Figure 3a illustrates the dependence of the EOD of skin at various instants of time during the interaction of the sample with the aqueous solution of ICG. One can clearly see that at the initial instant of time (0.5 min), the ICG absorption peaks against the background of the $A(\lambda)$ spectrum of skin are

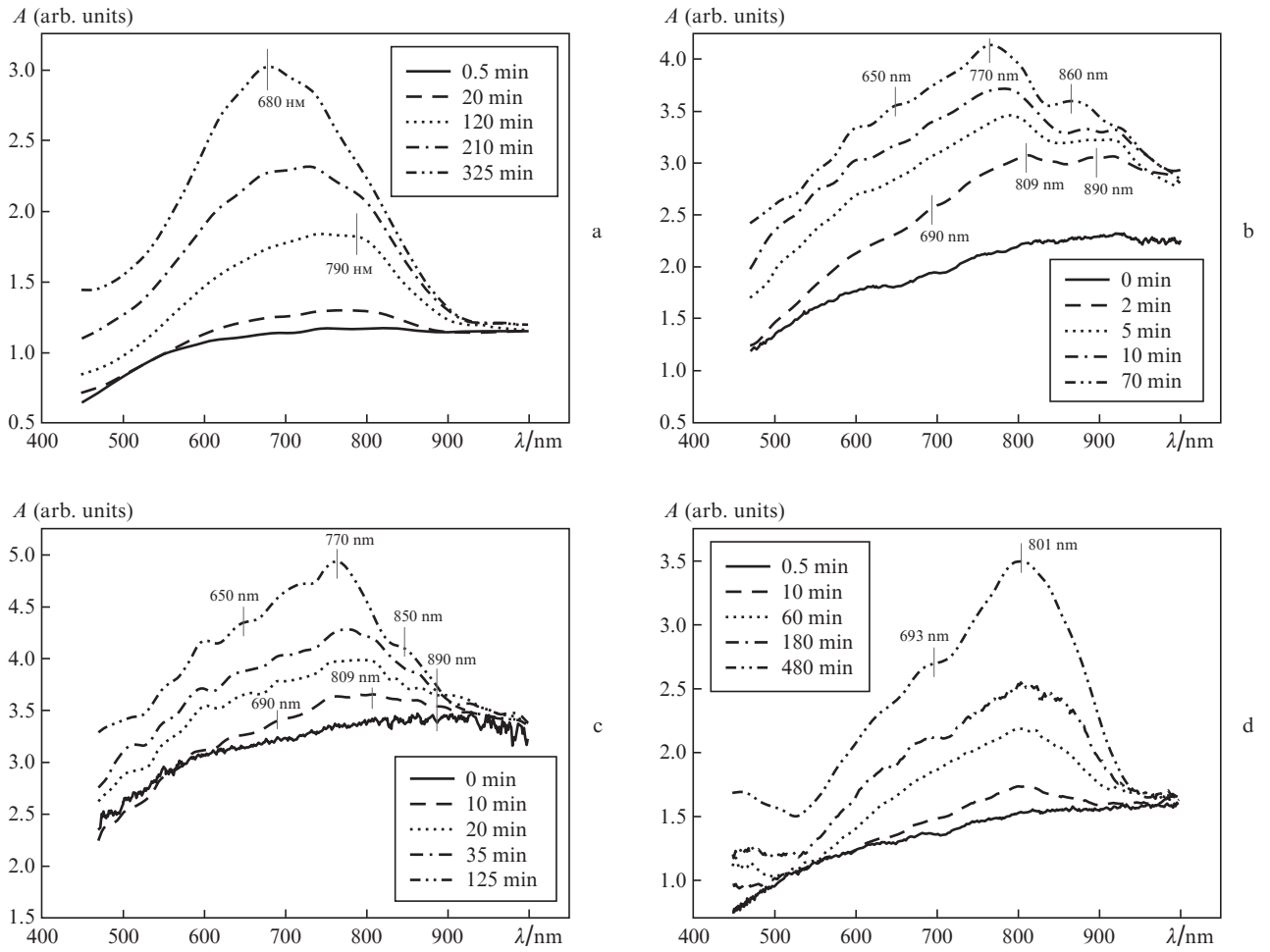

Figure 3. Changes in the spectra of the effective optical density of skin during its interaction with the ICG solution in (a) water, (b) 50% glycerol, (c) 50% propylene glycol and (d) 50% ethanol.

absent. Distortion of the shape of the EOD spectrum of skin is explained by an increased concentration of the dye due to diffusion. During the first 120 minutes of interaction of the dye solution with skin, the shape of the spectrum was significantly affected by the monomeric component of the ICG solution: The value of A at a wavelength of 790 nm was higher than that at a wavelength of 680 nm. With the passage of time, the peak at a wavelength of 680 nm became dominant, which corresponds, presumably, to an increase in the dye concentration in biological tissue and to its dimerisation. Perhaps, binding of the ICG molecules with collagen and dermis elastin improved the efficiency of dimerisation. A similar phenomenon was observed in the interaction of saline solutions of methylene blue and toluidine blue with cell membranes [38, 43]. An increase in the EOD in the short-wavelength region of the spectrum is also associated with the ICG influence.

Compared with the spectrum of the aqueous solution of ICG (see Fig. 2), the peak corresponding to the dimeric form of the dye is shifted to the short-wavelength region of the spectrum by 17 nm, whereas the second peak – by 21 nm to the long-wavelength region. Lowering of the peak, caused by the monomeric form of the dye (hypochromic effect), and the shift of the peak, associated with the dimeric form of the dye, to the short-wavelength region of the spectrum (hypsochromic effect) are typical not only for the interaction of the aqueous solution of ICG with the fibrous tissue of the dermis, but also for the interaction of water and saline solutions of other dyes (e.g., methylene blue and toluidine blue) with the cell biological tissue (mucosa) [38] and the colonies of bacteria [43].

The change in the position of the peaks, corresponding to the ICG absorption, in the EOD spectrum of skin as compared to their position in the absorption spectrum of the solution was observed in all these scenarios and caused by the interaction of the dye with the proteins of the dermis [23].

Figure 3b shows the spectral dependence of the EOD of skin at different instants of time during the interaction of the sample from the side of the dermis with ICG dissolved in 50% glycerol. Two minutes after the start of the interaction, the $A(\lambda)$ spectrum of skin clearly exhibited three bands resulting from the ICG absorption at the wavelengths of 690, 809 and 890 nm. These bands correspond to the absorption of dimers, monomers and J-aggregates of the dye, respectively. Compared with the ICG absorption spectra in 50% glycerol, the absorption maximum of dimers in the dermis is shifted to the short-wavelengths region by 34 nm, that of monomers – to longer wavelengths by 22 nm, and there appeared a peak corresponding to J-aggregates of molecules, which were absent in the solution. An increase in the EOD and change in the shape of the spectrum in the short-wavelength (450–500 nm) region, observed in the process

of ICG diffusion, is caused by the dye absorption band near 400 nm.

It should be noted that the process of diffusion is accompanied by a shift of the absorption band maxima in the short-wavelength region of the spectrum. 70 min after the start of the interaction, the absorption maximum of dimers was at the wavelength of 650 nm, of monomers – at 770 nm and of J-aggregates – at 860 nm.

Because the solvent used was a hyperosmotic immersion agent with a refractive index $n_{glyc} = 1.4$ (at 589 nm), it replaced the interstitial fluid; therefore, the refractive indices of collagen fibres of the dermis and the surrounding matrix became equal, which resulted in an increase in the transparency of biological tissue. A decrease in scattering made it possible to observe the appearance of two absorption bands of blood in the range from 500 to 600 nm within 10 min after the start of the interaction of the solution in question with the sample.

Thus, the spectra obtained are the result of rising absorption and decreasing scattering in biological tissue.

Figure 3c shows the spectral dependence of the EOD of skin at various instants of time during the interaction of the sample with ICG dissolved in 50% propylene glycol. The dynamics of changes in the position of the absorption peaks of monomeric, dimeric and polymeric forms of the dye is similar to the dynamics observed for the ICG solution in glycerol, except the fact that the peak corresponding to the J-aggregates of the dye is less pronounced. As in the case of 50% glycerol solution in water, predominant was the peak corresponding to the monomeric form of the dye. In the process of ICG diffusion we also observed a shift of the EOD maxima of all types of dye molecules by ~40 nm to the short-wavelength region of the spectrum. As a result of reducing the scattering due to diffusion of propylene glycol in the dermal tissue ($n_{prop} = 1.38$ at a wavelength of 589 nm), the absorption bands of blood in the region of 500–600 nm became noticeably pronounced within 20 min after the start of the interaction of the solution under study with the dermis.

The reasons behind a gradual shift to shorter wavelengths of the absorption bands of ICG dissolved in aqueous solutions of glycerol and propylene glycol are, apparently, associated with the process of optical clearing of skin. In this experimental geometry the observation was conducted on the side that is opposite to the surface through which the solutions in question experienced diffusion; therefore, the initially observed spectra became distorted due to scattering by skin. A gradual decrease in scattering, accompanying the diffusion of the dye, resulted in lower distortion.

Thus, when glycerol and propylene glycol are used as solvents, the ICG absorption maximum in the dermis is shifted during diffusion farther from the radiation wavelength of diode lasers (805 and 808 nm), which are employed for selective thermolysis [8, 29, 44], tissue welding [19, 45] or photodynamic effects [8, 16, 17, 29, 30]; this fact should be taken into account in order to increase the efficacy of procedures.

Figure 3d shows the spectral dependence of the EOD of skin at various instants of time during the interaction of the sample with ICG dissolved in 50% ethanol. The maximum EOD of ICG monomers in skin takes place at 801 nm (a shift by 14 nm to the long-wavelength region of the spectrum) and that of dimers – at 693 nm (a shift by 31 nm to the short-wavelength region). Unlike the dependences presented in Figs 3b and 3c, the position of the maxima in the EOD spectra during the ICG diffusion did not change, and no appreciable aggregation of the dye molecules was observed. More pronounced was the rise of the spectral curve at 450 nm. Prevailing during the entire observation time, as in the case of other alcoholic solutions, was the monomeric form of ICG. Since the optical clearing of biological tissue did not take place when use was made of ethanol as a solvent (the refractive index of ethanol $n_{eth} = 1.345$ at 589 nm is close to that of interstitial fluid $n_{flui} = 1.35$ [46]), the absorption bands of blood in the 500–600 nm region was not visualised and the spectrum shape was not distorted.

Table 1. Diffusion coefficients of ICG solutions in the dermis.

Solvent	Average thickness of samples/mm	Diffusion coefficient/ $cm^2\ s^{-1}$
Water	0.93±0.07	$(7.7\pm2.51)\times10^{-7}$
50% glycerol	0.66±0.04	$(1.0\pm0.3)\times10^{-8}$
50% propylene glycol	0.71±0.01	$(4.0\pm0.2)\times10^{-8}$
50% ethanol	0.80±0.01	$(1.88\pm0.3)\times10^{-6}$

The values of the ICG diffusion coefficients in the dermis are listed in Table 1 for various solvents. Since the EOD is determined from the experimentally measured backscattering coefficient of skin, this parameter depends on the structural and morphological characteristics of each sample. Variations in such characteristics as, for example, porosity of biological tissue, introduce an error in determining the diffusion rate of the dye into biological tissue. The variability of the optical parameters of the skin samples is no less than 10% [47] and, thus, introduces the greatest error in determining the effective optical density, and hence the diffusion coefficient of dye into the biological tissue. The data on the diffusion coefficients of dyes, including ICG, into biological tissues are virtually absent in the literature. Typical values for the diffusion coefficients of dyes in the solution lie in the range of 10^{-5}–10^{-6} $cm^2\ s^{-1}$ [48, 49]. One can see from Table 1 that when alcohol is added, the diffusion coefficient of the dye is 2.5 times higher than that of the aqueous solution of ICG. This is due to the ability of alcohol to increase the permeability of tissues for dyes and other agents [37, 50, 51]. The smallest value of the diffusion coefficient was observed when 50% glycerol was used as a solvent. A similar value of the diffusion coefficient was obtained with propylene glycol. Perhaps, slowing of diffusion in both cases is due to the fact that these solvents as hyperosmotic agents cause dehydration of biological tissue, resulting in compaction of the collagen matrix of the dermis. Formation of ICG J-aggregates in the dermis is, apparently, also related to the hindered diffusion of the dye.

4. Conclusions

By using backscattering spectroscopy we have studied diffusion of indocyanine green, dissolved in water and aqueous solutions of alcohols, into the dermis. The process of diffusion is found to be accompanied by a considerable (up to 40 nm) shift of the ICG absorption maximum in the dermis to the short-wavelength region of the spectrum and by the formation of an aggregated form of the dye when 50% aqueous solution of glycerol and propylene glycol are used as solvents.

During diffusion of ICG dissolved in ethanol, such an aggregation and a shift are not observed.

We have obtained the values of the diffusion coefficient of the dye in the dermis. Use of 50% ethanol as a solvent increases the diffusion coefficient of the dye by almost 2.5 times as compared with that of the aqueous solution. Glycerol and propylene glycol solvents, in contrast, slow diffusion of the dye.

The results obtained can be used to develop the methods of optical and optoacoustic imaging of skin, as well as for photothermal and photodynamic therapy, for tissue welding and other applications of laser surgery.

Acknowledgements. The study was supported by the RF President's Grants Council (State Support to the Leading Scientific Schools Programme, Grant No. NSh-703.2014.2).

The authors thank V.I. Kochubey and E.K. Volkova for assistance in the measurement of the transmission spectra of solutions.

References

1. Lammers T., Aime S., Hennink W.E., Storm G., Kiessling F. *Acc. Chem. Res*., **44**, 1029 (2011).
2. Khlebtsov N., Bogatyrev V., Dykman L., Khlebtsov B., Staroverov S., Shirokov A., Matora L., Khanadeev V., Pylaev T., Tsyganova N., Terentyuk G. *Theranostics*, **3**, 167 (2013).
3. Davis S.C., Pogue B.W., Dehghani H., Paulsen K.D. *Appl. Opt.*, **48**, D262 (2009).
4. Genina E.A., Fedosov I.V., Bashkatov A.N., Zimnyakov D.A., Al'tshuler G.B., Tuchin V.V. *Kvantovaya Elektron*., **38**, 263 (2008) [*Quantum Electron*., **38**, 263 (2008)].
5. Tong L., Wei Q., Wei A., Cheng J.-X. *Photochem. Photobiol*., **85**, 21 (2009).
6. Hama H., Kurokawa H., Kawano H., Ando R., Shimogori T., Noda H., Fukami K., Sakaue-Sawano A., Miyawaki A. *Nature Neuroscience, Tech. Report*, **14**, 1 (2011).
7. Kessentini S., Barchiesi D. *Biomed. Opt. Express*, **3**, 590 (2012).
8. Yanina I.Yu., Tuchin V.V., Navolokin N.A., Matveeva O.V., Bucharskaya A.B., Maslyakova G.N., Altshuler G.B. *J. Biomed. Opt.*, **17**, 058002 (2012).
9. Green F.J. *The Sigma-Aldrich Handbook of Stains, Dyes and Indicators* (Milwaukee: Aldrich Chem. Comp., Inc., 1990).
10. Axer-Siegel R., Lichter H., Rosenblatt I., Priel E., Yassur Y., Weinberger D. *Am. J. Ophthalmology*, **128**, 331 (1999).
11. Ciamberlini C., Guarnieri V., Longobardi G., Poggi P., Donati M.C., Panzardi G. *J. Biomed. Opt.*, **2**, 218 (1997).
12. Green H.A., Bua D., Anderson R.R., Nishioka N.S. *Arch. Dermatol*., **128**, 43 (1992).
13. Alacam B., Yazici B., Intes X., Chance B. *IEEE Trans. Biomed. Eng.*, **53**, 1861 (2006).
14. Philip R., Penzkofer A., Baumler W., Szeimies R.M., Abels C. *J. Photochem. Photobiol. A*, **96**, 137 (1996).
15. Alander J.T., Kaartinen I., Laakso A., Patila T., Spillmann T., Tuchin V.V., Venermo M., Valisuo P. *Intern. J. Biomed. Imaging*, **2012**, 940585 (2012).
16. Mamoon A.-M., Gamal-Eldeen A.M., Ruppel M.E., Smith R.J., Tsang T., Miller L.M. *Photodiag. Photodyn. Ther.*, **6**, 105 (2009).
17. Krespi Y.P., Kizhner V. *Lasers Surg. Med*., **43**, 187 (2011).
18. Tuchina E.S., Tuchin V.V., Khlebtsov B.N., Khlebtsov N.G. *Kvantovaya Elektron.*, **41**, 354 (2011) [*Quantum Electron*., **41**, 354 (2011)].
19. Rossi F., Matteini P., Ratto F., Menabuoni L., Lenzetti I., Pini R. *J. Biophoton.*, **1**, 331 (2008).
20. Babilas P., Shafirstein G., Baier J., Schacht V., Szeimies R.-M., Landthaler M., Baumler W., Abels C. *Lasers Surg. Med.*, **39**, 341 (2007).
21. Alam A., Chavan A.J., Flower R.W. https://www.google.com/patents/US6944493 (05.05.2014).
22. Kulyabina T.V. *Cand. Diss.* (Saratov, 2007).
23. Kochubey V.I., Kulyabina T.V., Tuchin V.V., Altshuler G.B. *Opt. Spektrosk*., **99**, 582 (2005).
24. Genina E.A., Bashkatov A.N., Kochubey V.I., Tuchin V.V., Altshuler G.B. *Pis'ma Zh. Tekh. Fiz*., **27**, 63 (2001).
25. Rotermund F., Weigand R., Penzkofer A. *Chem. Phys.*, **220**, 385 (1997).
26. Mauerer M., Penzkofer A., Zweck J. *J. Photochem. Photobiol. B*, **47**, 68 (1998).
27. Genina E.A., Bashkatov A.N., Sinichkin Yu.P., Kochubey V.I., Lakodina N.A., Altshuler G.B., Tuchin V.V. *J. Biomed. Opt.*, **7**, 471 (2002).
28. http://www.sigmaaldrich.com/content/dam/sigma-aldrich/docs/Sigma/Product_Information_Sheet/2/i2633pis.pdf (05.05.2014).
29. Tuchin V.V., Genina E.A., Bashkatov A.N., Simonenko G.V., Odoevskaya O.D., Altshuler G.B. *Lasers Surg. Med*., **33**, 296 (2003).
30. Genina E.A., Bashkatov A.N., Simonenko G.V., Odoevskaya O.D., Tuchin V.V., Altshuler G.B. *J. Biomed. Opt*., **9**, 828 (2004).
31. Mourant J.R., Johnson T.M., Los G., Bigio I.J. *Phys. Med. Biol*., **44**, 1397 (1999).
32. Austwick M.R., Woodhams J.H., Chalau V., Mosse C.A., Eliot C., Lovat L., Macrobert A.J., Bigio I.J., Bown S.J. *J. Innovative Opt. Health Sci.*, **4**, 97 (2011).
33. Lucassen G.W., van Veen G.N.A., Jansen J.A.J. *J. Biomed. Opt.*, **3**, 267 (1998).
34. Merzlyak M.N., Naqvi K.R. *J. Photochem. Photobiol. B*, **58**, 123 (2000).
35. Takiwaki H., Miyaoka Y., Arase S. *Skin Res. Technol.*, **10**, 130 (2004).
36. Zourabian A., Siegel A., Chance B., Ramanujan N., Rode M., Boas D.A. *J. Biomed. Opt*., **5**, 391 (2000).
37. Genina E.A., Kuzmina M.Yu., Pankov S.S., Bashkatov A.N., Tuchin V.V. *Proc. SPIE Int. Soc. Opt. Eng.*, **6535**, 65351H (2007).
38. Genina E.A., Bashkatov A.N., Chikina E.E., Tuchin V.V. *Biofiz*., **52**, 1104 (2007).
39. Levshin L.V., Saletskii A.M. *Teor. Eksper. Khim.*, **26**, 669 (1990).
40. Perel'man V.I. (Ed.) *Kratkii spravochnik khimika* (Concise Chemist's Handbook) (Moscow–Leningrad: Khimiya, 1964).
41. *Glycols*. Ed. by G.O. Gurme, F. Johnston (New York: Reinhold Publ. Corp., 1953).
42. Prahl S. http://omlc.ogi.edu/spectra/icg/index.html (01.03.2014).
43. Usacheva M.N., Teichert M.C., Biel M.A. *Lasers Surg. Med*., **29**, 165 (2001).
44. Chen W.R., Adams R.L., Higgins A.K., Bartels K.E., Nordquist R.E. *Cancer Lett.*, **98**, 169 (1996).
45. Athiraman H., Wolf R.F., Bartels K.E., Shivakoti S., Liu H., Chen W.R. *J. X-Ray Sci. Technol.*, **12**, 117 (2004).
46. Tuchin V.V. *Optical Clearing of Tissues and Blood* (Bellingham: SPIE Press, PM154, 2006).
47. Tuchin V.V. *Optika biologicheskikh tkanei. Metody rasseyaniya sveta v meditsinskoi diagnostike* (Optics of Biological Tissues. Light Scattering Methods in Medical Diagnostics) (Moscow: Fizmatlit, 2012).

48. Grigoriev I.S., Meilikhov E.Z. (Eds) *Handbook of Physical Quantities* (Boca Raton, FL: CRC Press, 1997; Moscow: Energoatomizdat, 1991).
49. Kotyk A., Janáček K. *Cell Membrane Transport. Principles and Techniques* (New York: Plenum Press, 1975; Moscow: Mir, 1980).
50. Genina E.A., Bashkatov A.N., Tuchin V.V. *Med. Laser Applicat.*, **23**, 31 (2008).
51. Mao Z., Zhu D., Hu Y., Wen X., Han Z. *J. Biomed. Opt*., **13**, 021104 (2008).